

PRELIMINARY NOTES

Mucociliary Clearance Mechanism in Smoking and Nonsmoking Normal Subjects

Toyoharu Isawa, Takeo Teshima, Tomio Hirano, Akio Ebina, and Kiyoshi Konno

The Research Institute for Chest Diseases and Cancer, Tohoku University, 4-1 Seiryomachi, Sendai 980, Japan

Mucociliary clearance mechanisms were evaluated in 17 normal subjects visually and qualitatively by radioaerosol inhalation cinescintigraphy of the lung, and quantitatively by calculating the following indices: (a) overall or regional lung retention ratio; (b) airway deposition ratio; (c) airway retention ratio; (d) airway clearance efficiency; and (e) alveolar deposition ratio. The inhaled aerosol deposited homogeneously throughout the lungs, and mucus transport was always cephalad in direction and constant in velocity, although a temporary stasis of mucus was seen in smokers. Overall lung retention ratio was significantly smaller and airway deposition ratio was significantly larger in the smokers than in nonsmokers, but there was no difference between the groups in airway retention ratio or airway clearance efficiency. There was an inverse relationship between alveolar deposition ratio and cigarette consumption. Mucociliary clearance mechanisms were well maintained in the normal subjects, but in the smokers inhaled aerosol tended to deposit more proximally.

J Nucl Med 25: 352-359, 1984

Cinematographic display of the lung images following radioaerosol inhalation is useful for the visual and qualitative assessment of mucociliary clearance mechanisms in the lungs (1-3). Using this method we have learned, initially, that mucus transport in the airways is highly protean in direction and pattern according to underlying pathology (1-3), but what is within normal limits and what is not in this newly developed modality has not been established. Indices to quantify mucociliary clearance mechanisms in the lungs have not been determined.

The purpose of the present study was to see whether there was any visual difference in mucociliary clearance mechanisms in normal subjects, currently smoking and nonsmoking, or in ex- and nonsmokers, and to define indices to quantify the airway clearance mechanisms in the lungs.

MATERIALS AND METHODS

Seventeen healthy male physician colleagues who were actively engaged in daily patient care and research, volunteered for this study. Their ages ranged from 29 to 51 yr, with an average 34.

They had no history of pulmonary disease, and their chest radiographs were within normal limits. They had no abnormalities of pulmonary function, as shown in Table 1. At the time of study they had no acute illness such as sore throat or bronchitis. Three were ex-smokers, five nonsmokers, and nine smokers (Table 1). Ex-smokers had a cigarette-smoking history of 2 to 9 pack yr, but they had stopped smoking for more than 10 yr. Smokers abstained from smoking for at least 2 hr before radioaerosol inhalation, but smoking was permitted from 2 hr after aerosol inhalation.

Each subject inhaled ultrasonically generated Tc-99m human serum albumin aerosol (mass median diameter 3.73 μm , with geometric s.d. 1.73) (4) for less than 2 min, by tidal breathing through a mouthpiece with the nose clipped; he immediately lay supine comfortably on

Received Feb. 9, 1983; revision accepted Sept. 19, 1983.

For reprints contact: Toyoharu Isawa, MD, Dept. of Medicine, The Research Institute for Chest Diseases and Cancer, Tohoku University, 4-1 Seiryomachi, Sendai 980, Japan.

TABLE 1. LUNG FUNCTION DATA AND SMOKING HISTORY OF THE NORMAL SUBJECTS STUDIED

| Subject no. | Age | Vital capacity (ml) | % Predicted (%) | FEV _{1.0} % (%) | MMF [†] (l/sec) | V ₅₀ [‡] (l/sec) | V ₂₅ [§] (l/sec) | Smoking status | | Packs day | Pack-yr |
|-------------|-----|---------------------|-----------------|--------------------------|--------------------------|--------------------------------------|--------------------------------------|-----------------|-----------------|-----------|---------|
| | | | | | | | | started at age: | stopped at age: | | |
| 1 | 43 | 4699 | 124 | 86 | 5.21 | 7.20 | 1.00 | 18 | 31 | 0.5 | 7 |
| 2 | 34 | 3824 | 99 | 72 | 1.91 | 3.20 | 0.80 | 18 | 24 | 1.5 | 9 |
| 3 | 32 | 4929 | 110 | 89 | 5.95 | 8.00 | 4.00 | 18 | 22 | 0.5 | 2 |
| 4 | 29 | 4832 | 120 | 78 | 3.71 | 4.43 | 1.47 | | | 0 | 0 |
| 5 | 29 | 4699 | 118 | 86 | 4.91 | 6.60 | 2.20 | | | 0 | 0 |
| 6 | 30 | 4595 | 112 | 81 | 4.12 | 5.30 | 1.50 | | | 0 | 0 |
| 7 | 31 | 4384 | 103 | 91 | 4.86 | 5.40 | 2.20 | | | 0 | 0 |
| 8 | 40 | 4186 | 110 | 88 | 5.77 | 6.10 | 2.70 | | | 0 | 0 |
| 9 | 36 | 4078 | 106 | 75 | 3.28 | 3.73 | 1.21 | 20 | | 1.5 | 24 |
| 10 | 33 | 3942 | 100 | 84 | 3.20 | 4.00 | 1.20 | 19 | | 1.0 | 14 |
| 11 | 32 | 3689 | 91 | 81 | 2.86 | 3.00 | 0.80 | 20 | | 1.5 | 18 |
| 12 | 37 | 4123 | 101 | 81 | 3.39 | 4.20 | 1.00 | 20 | | 1.5 | 26 |
| 13 | 28 | 3654 | 92 | 93 | 5.61 | 7.20 | 2.40 | 23 | | 2.0 | 10 |
| 14 | 34 | 3802 | 96 | 83 | 4.27 | 5.80 | 1.50 | 18 | | 1.5 | 24 |
| 15 | 51 | 3670 | 103 | 82 | 3.19 | 3.80 | 1.00 | 18 | | 1.5 | 50 |
| 16 | 38 | 4036 | 103 | 76 | 2.56 | 3.00 | 0.90 | 20 | | 1.0 | 18 |
| 17 | 29 | 4490 | 105 | 89 | 5.70 | 6.80 | 2.60 | 20 | | 1.0 | 9 |

* FEV_{1.0}%: Forced expiratory volume in 1 sec/forced vital capacity in percentage.

† MMF: maximal mid-expiratory flow rate.

‡ V₅₀: maximum flow at 50% vital capacity.§ V₂₅: maximum flow at 25% vital capacity.

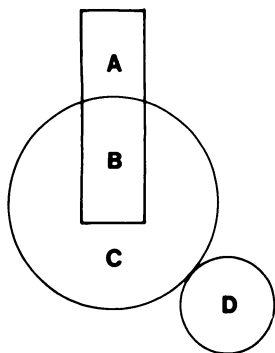


FIG. 1. Diagram of aerosol deposition sites. (A) extrapulmonary ciliated airways, (B) intrapulmonary ciliated airways, (C) nonciliated distal airways and/or alveolar space, (D) stomach or GI tract.

the bed under a gamma camera and the resulting deposition pattern and clearance were monitored continuously over the entire thorax for 2 hr in 16 of the 17 subjects. In the remaining normal subject, radioactivity was measured for the first 15 min only. Special care was taken to keep subjects in the same supine position during the 2-hr monitoring period. The total radioactivity initially deposited in the thorax was from 2.0 to 3.0 mCi. Twenty-four hours later, 9 of the 17 subjects were monitored again for 15 min. None coughed during the measurements. Every 10 sec, data were stored in a computer in frame mode with 64 × 64 matrix.

The data stored were retrieved and utilized in two ways: (a) the 720 10-sec frames were edited by pulmonary cinescintigraphy (1-3) for visual evaluation of mucociliary clearance; and (b) the following indices, defined below, were calculated: overall lung retention ratio, airway deposition ratio, airway retention ratio, airway clearance efficiency, and alveolar deposition ratio.

As shown diagrammatically in Fig. 1, when a radioaerosol is inhaled, radioactivity deposits in the extrapulmonary ciliated airways (A), intrapulmonary ciliated airways (B), in the nonciliated small distal airways and/or the alveoli (C) or, by being swallowed, in the stomach and/or the GI tract (D). Disregarding the radioactivity in the stomach (D), the radioactivity in each compartment at time zero can be written as follows:

$$A_0 + B_0 + C_0 = T_0, \quad (1)$$

where A, B, and C represent the compartments as in Fig. 1, and T, the total radioactivity in all three. At time t, radioactivity at each compartment would be

$$A_t + B_t + C_t = T_t. \quad (2)$$

If radioactivity is corrected for physical decay, the formula (2) becomes

$$A_{tc} + B_{tc} + C_{tc} = T_{tc}, \quad (3)$$

which can conveniently define the net radioactivity re-

maining in the right and left lungs at 24 hr after radioaerosol inhalation. It is equivalent to the radioactivity initially deposited in Compartment C (nonciliated distal airways and alveolar space), because at 1 day this area has not been cleared (5-8). If we let C_0 = net radioactivity at 24 hr, corrected for physical decay, then $C_{tc} = C_0$, and

$$A_{tc} + B_{tc} + C_0 = T_{tc}. \quad (4)$$

Practically speaking, however, it was extremely difficult to measure A without its being contaminated by swallowed radioactivity remaining in the esophagus. In the calculation of the indices, therefore, radioactivity in the extrapulmonary compartment was neglected, in which case the formulae become:

$$B_0 + C_0 = T_0 \quad (1')$$

$$B_t + C_t = T_t \quad (2')$$

$$B_{tc} + C_0 = T_{tc}. \quad (3')$$

The indices are then defined as follows:

Overall lung retention ratio (%) = $T_{tc}/T_0 \times 100$. This ratio expresses the amount of radioactivity remaining in the lungs at time t relative to the total radioactivity initially deposited. A regional lung retention ratio is similarly defined as the amount of regional radioactivity divided by the total radioactivity initially deposited in that region.

Airway deposition ratio (%) = $B_{tc}/T_0 \times 100 = (T_{tc} - C_0)/T_0 \times 100$. This is therefore the overall lung retention ratio - alveolar deposition ratio, and it indicates the amount of radioactivity throughout the ciliated airways relative to the total radioactivity initially deposited in both lungs.

Airway retention ratio (%) = $B_{tc}/B_0 \times 100 = (T_{tc} - C_0)/(T_0 - C_0) \times 100$ (%). This ratio indicates what percentage of radioactivity initially deposited on the ciliated airways still remains there at time t.

Airway clearance efficiency (%) = $(B_0 - B_{tc})/B_0 \times 100 = (T_0 - T_{tc})/(T_0 - C_0) \times 100 = 100 - \text{airway retention ratio}$. This indicates what percentage of the radioactivity deposited on the ciliated airways has already been cleared by time t.

Alveolar deposition ratio (%) = $C_0/T_0 \times 100$ (%). This is the percentage of the total initial radioactivity that remains at 24 hr.

These indices were calculated for each 10-min period and compared with the radioactivity in the initial 10-min period. As the measurement of radioactivity at 24 hr could not be made in exactly the identical position—that is, in the identical pixel-to-pixel relationship to the initial measurement for 2 hr—we did not try to evaluate these indices in the form of image data by subtracting and/or dividing the corresponding images. We simply calculated these indices numerically by using the physically corrected T_0 , T_{tc} , and C_0 , which were measurable.

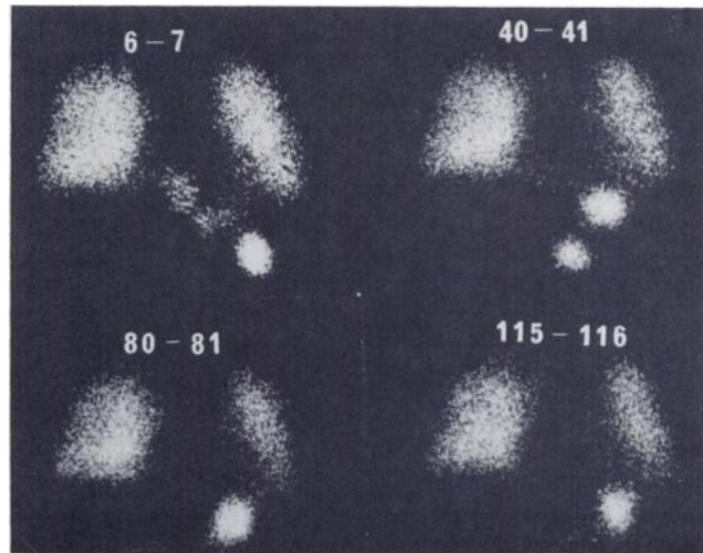


FIG. 2. Aerosol inhalation lung images in 29-yr-old nonsmoking normal subject. Each 1-min lung image was made between indicated times after aerosol inhalation. Note homogeneous intrapulmonary aerosol deposition, and faint radioactivity in lower esophagus and stomach.

To calculate these indices, the lung contour had to be determined. This was defined by light pen on the 24-hr display after subtracting the background radioactivity, so that the right and left lungs became barely separated at the anterior mediastinum. The initial lung contour immediately after aerosol inhalation was constructed after the 24-hr lung contour, so that at least the numbers of pixels concerned were not different from each other by more than 2%. When a 24-hr study was not done, the lung contour was arbitrarily demarcated by light pen so that the edge of the lung corresponded to approximately 2% to 3% of the initial maximum count rate in the lungs, since this is the normal relationship when a 24-hr count can be done. When regional lung retention ratios were calculated, seven regions of interest (ROIs) were usually selected: the entire right and left lungs separately, the upper halves of the right and left lungs, the right lower half, and two peripheral lung regions covering peripheral bands of width approximately one fourth of the transverse diameter of each lung. To calculate the retention ratio for these peripheral lung regions, the data for the right and left peripheral ROIs were lumped together.

Student's *t*- and paired *t*-tests were used for statistical analysis. The results were considered significant if the *p* value was less than 0.05 (9). Curve-fitting techniques were applied to all the data pairs, and coefficients of determination, r^2 , and regression coefficients were calculated for experimental formulae of the forms $y = a + bx$, $y = ae^{bx}$, $y = a + b \cdot \ln x$ and $y = ax^b$. The regression curve with the largest value of r^2 was considered the best fit.

RESULTS

Lung function data. Vital capacity in all subjects was over 91% of the predicted (10) as shown in Table 1, and

there was no significant statistical difference between smokers and non- and ex-smokers in percent forced expiratory volume in 1 sec ($FEV_{1.0\%}$), in maximal mid-expiratory flow (MMF), or in maximal expiratory flow either at 50% (\dot{V}_{50}) or 25% (\dot{V}_{25}) vital capacity (11).

Radioaerosol inhalation lung cinescintigraphy

In the four nonsmokers and two of the three ex-smokers, transport of radioactivity in the trachea was always cephalad in direction, steady in its progress, and showed no stagnation of radioactivity in the bronchi or trachea. Since cinescintigraphy cannot be used in print to illustrate mucociliary clearance mechanisms, we present several static images in Fig. 2 as a better-than-nothing substitute.

In all the smokers and one ex-smoker (No. 2), although radioactive transport was still cephalad in direction and motion nearly constant, temporary collections of radioactivity could be seen over the bronchi near the carina or over the trachea. Otherwise there was essentially no visible difference in tracheal radioactive transport between the smokers and the non- or ex-smokers. All the subjects showed a homogeneous aerosol deposition in the lungs (Fig. 2), and no difference was appreciable in regional patterns of clearance from the lung parenchyma. Any deviation from the above findings will be taken as abnormal.

Overall and regional lung retention ratios. Because of the foregoing lack of difference, the data of the ex-smokers and the nonsmokers were lumped together and these people are referred to as the nonsmoking normal subjects. Overall lung retention ratios were smaller in the smoking normal subjects than in the nonsmoking counterparts, as shown in Fig. 3. Analysis by curve-fitting techniques indicated that the former are described best by y (overall lung retention ratio) = $119.96 - 11.47 \cdot \ln x$ (min) ($r^2 = 0.73$, $p \ll 0.001$), and the latter by $y = 110.33 - 6.52 \cdot \ln x$ (min) ($r^2 = 0.58$, $p \ll 0.001$).

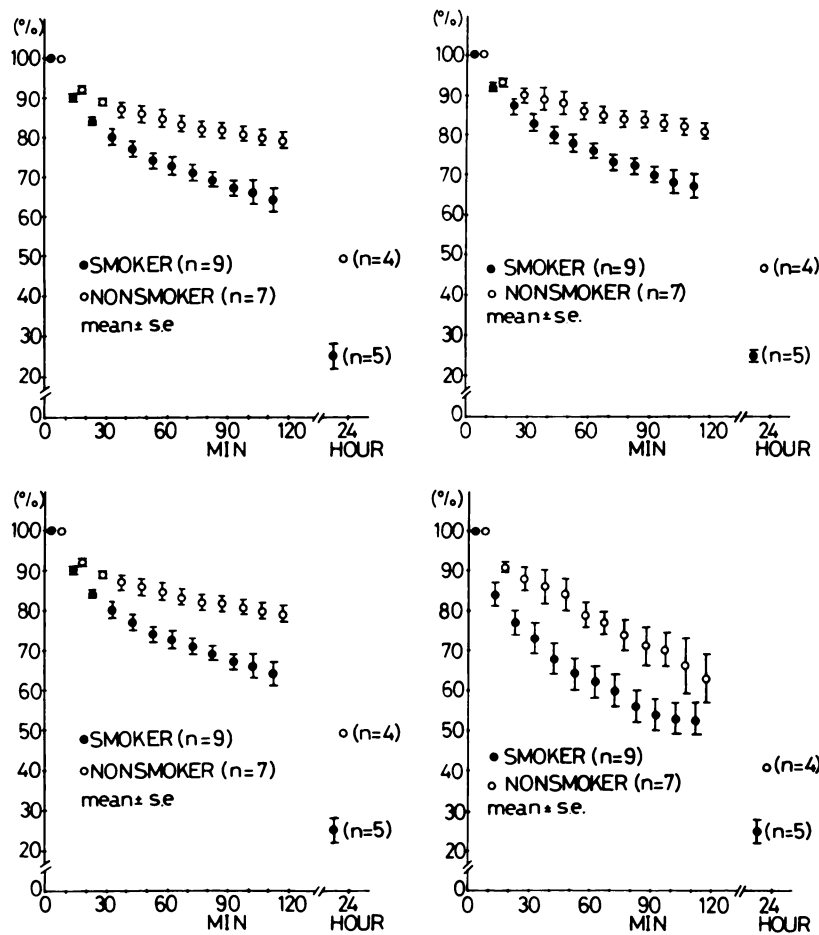


FIG. 3. Overall and regional lung retention ratios in smoking and nonsmoking subjects: (upper left) overall, (upper right) in right lung, (lower left) in upper half of right lung, and (lower right) in lung periphery. Difference between smoking and nonsmoking normal subjects is statistically significant at 30 min and thereafter ($p \leq 0.05$).

Regional lung retention ratios were also significantly smaller in any lung region in the smoking normal subjects compared with those in the nonsmoking group (Fig. 3).

Airway deposition ratios. Airway deposition ratios were significantly smaller in the nonsmoking than in the smoking normal subjects in the first hour following inhalation of radioaerosol (Fig. 4), indicating a better penetration of inhaled aerosol in the former into the nonciliated distal airways and/or alveoli. Analysis by curve-fitting techniques indicated that the smoking normal subjects are fitted best by y (airway deposition ratio) = $94.75 - 11.52 \cdot \ln x$ (min) and the nonsmoking to $y = 61.83 - 6.12 \cdot \ln x$ (min), with $r^2 = 0.52$ ($p \ll 0.001$) and 0.61 ($p \ll 0.001$), respectively.

Airway retention ratios. These were not significantly different between the smoking and nonsmoking groups as shown in Fig. 5, although the former tended to indicate smaller ratios. Analysis by curve-fitting indicated that the former are fitted best by y (airway retention ratio) = $126.73 - 15.93 \cdot \ln x$ (min) and the latter by $y = 116.44 - 11.41 \cdot \ln x$ (min), with $r^2 = 0.63$ ($p \ll 0.001$) and 0.58 ($p \ll 0.001$), respectively.

Airway clearance efficiency. As shown in Fig. 6, airway clearance efficiencies were not statistically different between the smoking and the nonsmoking subjects. As

a whole, airway clearance efficiency is fitted best by y (airway clearance efficiency) = $-23.03 + 14.06 \cdot \ln x$ (min), with $r^2 = 0.60$ ($p < 0.001$).

Alveolar deposition ratios. The alveolar deposition ratios were measured in five smoking and four nonsmoking normal subjects, and are plotted in Fig. 7 against the amount of cigarette consumption in pack-yr. As the

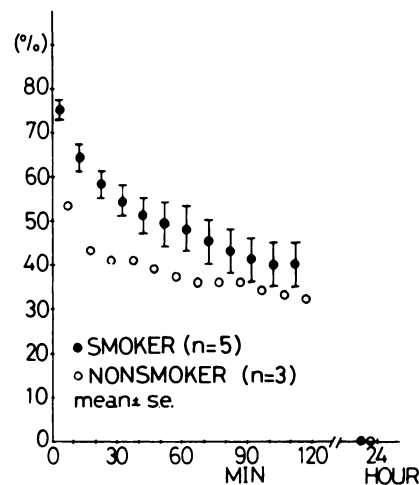


FIG. 4. Airway deposition ratio. Difference between smoking and nonsmoking normal subjects is statistically significant until 60 min ($p \leq 0.05$) but is not significant thereafter.

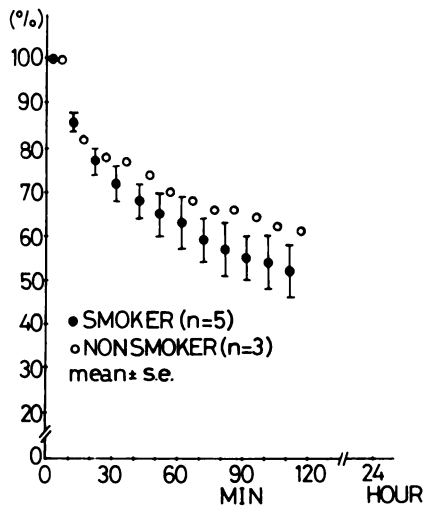


FIG. 5. Airway retention ratio. Difference between smoking and nonsmoking normal subjects is not significant.

amount of cigarette consumption increased, the alveolar deposition ratios decreased in a dose-related fashion: y (alveolar deposition ratio) = $46.83 - 0.69x$ (pack-yr) ($r^2 = 0.68, p < 0.01$). The alveolar deposition ratios were significantly different between the smoking and the nonsmoking group, with the former showing definitely smaller alveolar deposition ratios ($p < 0.001$). The mean alveolar deposition ratio in those nine normal subjects was 35.8 ± 13.1 (mean \pm s.d.) %.

DISCUSSION

In our normal subjects we did not observe any retrograde migration or retreat, stasis or stagnation of puddling of mucus, frequent up-and-down motions of radioactive globs in the trachea or bronchi, or migration into the opposite bronchus, as is seen in patients with obstructive airways disease or bronchogenic carcinoma (1-3). In the normal, aerosol deposition was homogeneous throughout the lungs (Fig. 2) (12), and the transport of airway mucus was always cephalad in direction and steady in progression, in contrast to the temporary stasis of puddling of mucus often seen in the trachea in smokers. Such stasis, however, never persisted long. It was impossible to tell normal smokers from nonsmoking normals by simply looking at aerosol inhalation lung cinescintigrams, but we can distinguish normal subjects by this means from patients with obstructive airways disease or bronchogenic carcinoma (1-3). Anyway the visual evaluation of mucociliary clearance by this cinescintigraphic method seems to offer a new dimension in the study of pulmonary medicine, especially in the evaluation of this aspect of nonrespiratory lung function. The tracheal mucociliary transport rate has been shown to correlate with the intrapulmonary mucociliary clearance (13), and similar transport mechanisms must be taking place in the large airways and in the intrapulmonary ciliated airways.

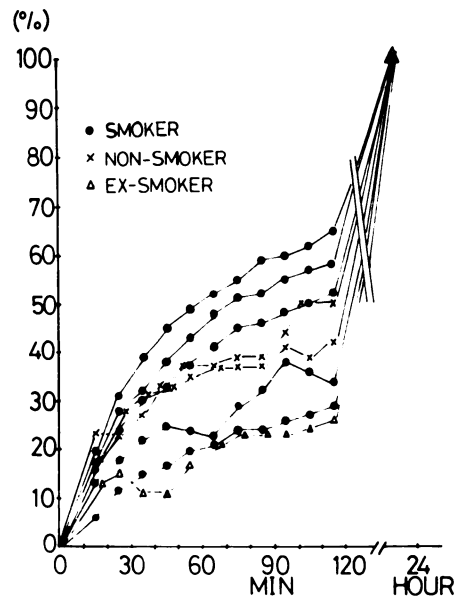


FIG. 6. Airway clearance efficiency. Difference between smoking and nonsmoking normal subjects is not significant.

In this study the data obtained from the normal subjects were utilized also for numerical assessment of mucociliary clearance function, besides providing for inhalation lung cinescintigraphy. As shown in Fig. 3, not only overall but regional lung retention ratios were significantly smaller in the smoking normal subjects than in their nonsmoking counterparts, giving the impression that airway clearance is faster in the former than in the latter. Albert et al. (5,14,15), and Camner et al. (16), report an accelerating effect of cigarette smoking on clearance rates. Conflicting results have also been reported: slower clearance (17,18) or no difference in clearance rates (19-21). As far as the lung retention ratios are concerned, our results appear to support the seemingly accelerated clearance.

A decrease in ciliary beating frequency, and even stasis of cilia, on exposure to cigarette smoke have been demonstrated in animal experiments (14,22-27). With

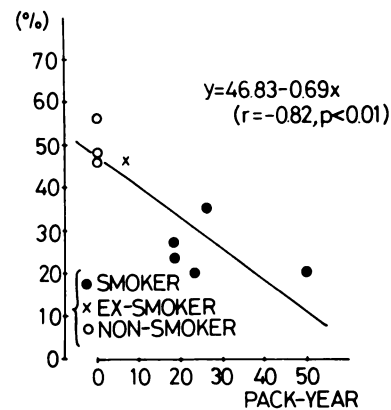


FIG. 7. Alveolar deposition ratio plotted against amount of smoking in pack-yr. There is significant linear correlation. Alveolar deposition ratio (%) = $46.83 - 0.69 \times \text{pack-yr}$ ($r = -0.82, p < 0.01$).

these findings in mind, whether mucociliary clearance is truly accelerated in smoking normal subjects is a question. Albert and others think that this is not due to an increased ciliary beat rate but rather to increased mucus production (5).

If we take into consideration the amount of radioactivity remaining in the lungs at 24 hr after aerosol inhalation, and define it as aerosol deposited in the alveoli or at least in the nonciliated distal air spaces where mucociliary clearance mechanisms are not operative (5-8), neither the airway retention ratios nor the airway clearance efficiencies as we define them were different between the smoking normal subjects and the non-smoking counterparts, indicating that aerosol deposited on the ciliated airways is cleared with similar efficiencies in both groups. Clearance is not actually accelerated in the former. In this sense overall or regional lung retention ratios alone could be misleading. Airway deposition ratios, however, are significantly higher in the smokers, and naturally their alveolar deposition ratios are significantly smaller. All these indices confirm the findings that in smokers inhaled aerosol has deposited more proximally on the ciliated airways than in the nonsmoking normal subjects (28-30). There is even an inverse relationship between the amount of cigarette smoking in pack-yr and the alveolar deposition ratios. From the regression line in Fig. 7, the alveolar deposition ratios can be estimated in a person with normal lung function, and all the indices described here could even be calculated without repeating the measurement at 24 hr.

As Albert and others believe, the rate of bronchial clearance could be partly a function of mucus production (5). Even asymptomatic healthy smokers could develop some subclinical airway mucosal changes such as respiratory bronchiolitis, increases in mural inflammatory cells and denuded epithelium (31), goblet-cell hyperplasia (32), or increases in ciliated, mucous, and basal cells (33). Even the microscopic structure of cilia seems to be affected by chronic exposure to cigarette smoke (34). Not only the quantity but also the quality of secreted mucus could well be affected by cigarette smoking. All these factors must potentially lead to a subclinical bronchoconstriction in normal smokers, although conventional lung function data remain within normal limits. If we analyze aerosol inhalation studies, as we did here in normal subjects with normal lung function data, we will surely be able to tell smokers from nonsmoking normal subjects.

Aerosol of a larger particle size, or an increased downward velocity of the aerosol, are important factors in determining the site of deposition (4,5). Our particle size compares well with that used by others (17,18).

When calculating the various indices described here, we had a problem with the extrapulmonary airways. Abnormalities of mucus transport that we can appreciate with our lung cine-scintigraphy are mostly in the trachea

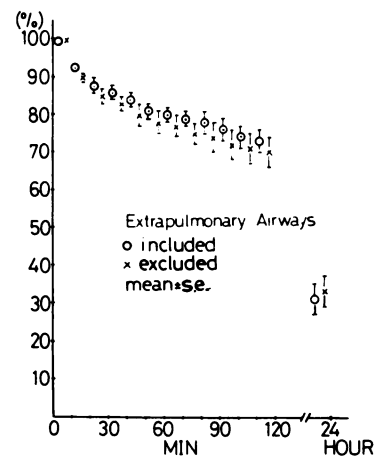


FIG. 8. Overall lung retention ratios when radioactivity in extrapulmonary airways is included or excluded from calculation of ratio. No statistical difference is seen in these normal subjects ($n = 16$).

and the major bronchi, where radioactivity in the surrounding lung tissue does not interfere. Theoretically we should incorporate radioactivity in the whole thorax, including that in the extrapulmonary airways, in the calculation of the indices. The greatest obstacle against doing so is the difficulty in eliminating radioactivity in the esophagus, which is brought up from the extrapulmonary airways and swallowed. By looking at the cine-scintigrams, however, we can appreciate the rising radioactivity in the trachea or bronchi and its downward movement in the esophagus. In normal subjects there was no statistical difference either by Student's t-test or paired t-test in overall lung retention ratio, whether the radioactivity in the extrapulmonary airway was included in the calculation or excluded, as shown in Fig. 8, but to cope with the data from esophageal contamination, which we cannot assess by merely counting the radioactivity, we propose to disregard extrapulmonary radioactivity in the calculation of these indices. In spite of this, radioaerosol inhalation lung cine-scintigraphy is useful for a visual and qualitative evaluation of the actual dynamic mucociliary clearance mechanisms, and the indices described here are convenient for a quantitative assessment of the mucociliary clearance in the lungs.

ACKNOWLEDGMENTS

The authors thank our colleagues who willingly volunteered for this study, Dr. Hiroshi Ogawa of the Daiichi Radioisotope Laboratories for his generous supply of human serum albumin kits, and Ms. Shoko Sakamoto for her clerical assistance in preparing the manuscript.

REFERENCES

1. ISAWA T, TESHIMA T, HIRANO T, et al: Radioaerosol inhalation lung cine-scintigraphy: a preliminary report. *Tohoku J Exp Med* 134:245-255, 1981
2. KONNO K, ISAWA T, TESHIMA T, et al: Aerosol cine-scintigraphy for evaluation of non-respiratory lung function. *Jpn J Med* 20:293, 1981

3. ISAWA T, TESHIMA T, HIRANO T, et al: Radioaerosol inhalation lung cine-scintigraphy in health and disease. In *Nuclear Medicine and Biology*. Proceedings of the Third World Congress of Nuclear Medicine and Biology, Raynaud C, ed. Paris, Pergamon 1982, pp 2026-2028
4. TESHIMA T, ISAWA T, HIRANO T, et al: Measurement of aerosol size and its effect on inhaled aerosol deposition patterns in the lungs. *Jpn J Nucl Med* 18:449-454, 1981
5. ALBERT RE, LIPPMANN M, PETERSON HT JR, et al: Bronchial deposition and clearance of aerosols. *Arch Intern Med* 131:115-127, 1973
6. MORROW PE: Alveolar clearance of aerosols. *Arch Intern Med* 131:101-108, 1973
7. GREEN GM: Alveolobronchiolar transport mechanisms. *Arch Intern Med* 131:109-114, 1973
8. POE ND, COHEN MB, YANDA RL: Application of delayed lung imaging following radioaerosol inhalation. *Radiology* 122:739-746, 1977
9. SWINSCOW TDV: *Statistics at Square One*. 2nd Ed. London, British Medical Association, 1977
10. BALDWIN ED, COURNAND A, RICHARD DW JR: Pulmonary insufficiency. I. Physiological classification, clinical methods of analysis, standard values in normal subjects. *Medicine* 27:243-278, 1948
11. CHERNIACK RM, RABER MB: Normal standards for ventilatory function using an automated wedge spirometer. *Am Rev Respir Dis* 106:38-46, 1972
12. ISAWA T, WASSERMAN K, TAPLIN GV: Lung scintigraphy and pulmonary function studies in obstructive airway disease. *Am Rev Respir Dis* 102:161-172, 1970
13. YEATES DB, PITT BR, SPEKTOR DM, et al: Coordination of mucociliary transport in human trachea and intrapulmonary airways. *J Appl Physiol* 51:1057-1064, 1981
14. ALBERT RE, SPIEGELMAN JR, SHATSKY S, et al: The effect of acute exposure to cigarette smoke on bronchial clearance in the miniature donkey. *Arch Environ Health* 18:30-41, 1969
15. ALBERT RE, PETERSON HT JR, BOHNING DE, et al: Short-term effects of cigarette smoking on bronchial clearance in humans. *Arch Environ Health* 30:361-367, 1975
16. CAMNER P, PHILIPSON K, ARVIDSSON T: Cigarette smoking in man. Short-term effect on mucociliary transport. *Arch Environ Health* 23:421-426, 1971
17. LOURENÇO RV, KLIMEK MF, BOROWSKI CJ: Deposition and clearance of 2μ particles in the tracheobronchial tree of normal subjects—smokers and nonsmokers. *J Clin Invest* 50:1411-1420, 1971
18. CAMNER P, PHILIPSON K: Tracheobronchial clearance in smoking-discordant twins. *Arch Environ Health* 25:60-63, 1972
19. YEATES DB, ASPIN N, LEVISON H, et al: Mucociliary tracheal transport rates in man. *J Appl Physiol* 39:487-495, 1975
20. LUCHSINGER PC, LAGARDE B, KILFEATHER JE: Particle clearance from the human tracheobronchial tree. *Am Rev Respir Dis* 97:1046-1050, 1968
21. THOMSON ML, PAVIA D: Long-term tobacco smoking and mucociliary clearance from the human lung in health and respiratory impairment. *Arch Environ Health* 26:86-89, 1973
22. DALHAMN T: Studies on tracheal ciliary activity. Special reference to the effect of cigarette smoke in living animals. *Am Rev Respir Dis* 89:870-877, 1964
23. DALHAMN T: The anticiliostatic effect of cigarettes treated with oxolamine citrate. *Am Rev Respir Dis* 99:447-448, 1969
24. KAMINSKI EJ, FANCHER OE, CALANDRA JC: In vivo studies of the ciliastatic effect of tobacco smoke. Absorption of ciliastatic components by wet surfaces. *Arch Environ Health* 16:188-193, 1968
25. HOLMA B: The acute effect of cigarette smoke on the initial course of lung clearance in rabbits. *Arch Environ Health* 18:171-173, 1969
26. IRAVANI J: Effects of cigarette smoke on the ciliated respiratory epithelium of rats. *Respiration* 29:480-487, 1972
27. ISAWA T, HIRANO T, TESHIMA T, et al: Effect of non-filtered and filtered cigarette smoke on mucociliary clearance mechanism. *Tohoku J Exp Med* 130:189-197, 1980
28. DOLOVICH MB, SANCHIS J, ROSSMAN C, et al: Aerosol penetrance: a sensitive index of peripheral airways obstruction. *J Appl Physiol* 40:468-471, 1976
29. PAVIA D, THOMSON M, SHANNON HS: Aerosol inhalation and depth of deposition in the healthy lung. The effect of airway obstruction and tidal volume inhaled. *Arch Environ Health* 32:131-137, 1977
30. GARRARD CS, GERRITY TR, SCHREINER JF, et al: Analysis of aerosol deposition in the healthy human lung. *Arch Environ Health* 36:184-193, 1981
31. NIEWOEHNER DE, KLEINERMAN J, RICE DB: Pathologic changes in the peripheral airways of young cigarette-smokers. *N Engl J Med* 291:755-758, 1974
32. LAMB D, REID L: Goblet cell increase in rat bronchial epithelium after exposure to cigarette and cigar tobacco smoke. *Br Med J* 1:33-35, 1969
33. JEFFERY PK, REID LM: The effect of tobacco smoke, with or without phenylmethyloxadiazole (PMO), on rat bronchial epithelium: a light and electron microscopic study. *J Pathol* 133:341-359, 1981
34. AILSBY RL, GHADIALLY FN: Atypical cilia in human bronchial mucosa. *J Pathol* 109:75-78, 1973
35. TAPLIN GV, TASHKIN DP, CHOPRA SK, et al: Early detection of chronic obstructive pulmonary disease using radionuclide lung imaging procedures. *Chest* 71:567-575, 1977